COUPLED ANALYSIS OF THE DOUBLE SUBMERGED ARC WELDING PROCESS USING ELEMENT MOVEMENT TECHNIQUES

Birsan Dan Catalin[1], Mircea Octavian[1]

[1] *"Dunarea de Jos" University, Dan.Birsan@ugal.ro*

Abstract: *The welds of thick plates are, preferable, performed by submerged arc welding procedure (SAW) with multiple arcs in order to increase the productivity and to achieve better mechanical properties of the welded joints. This research focuses on theoretical investigations of temperatures field in the welded joints achieved by double SAW process on ordinary steel. The authors developed a 3D model for the coupled finite element analysis of butt-joint using double SAW procedure, in distinct melted pools. Finally, numerical results on the temperature field are analysed and discussed and important conclusions are drawn.*

Keywords: *finite element, welding process, SAW*

1. Introduction

The heat transfer has a major influence on the metallurgical and mechanical properties of the steels welds. The most interesting regions in the analysis of heat transfer are the fusion zone (FZ) and heat affected zone (HAZ), where high temperatures are reached and, further, lead to phase transformations and alterations of the mechanical properties of the welds. For this reason a numerical investigation of the temperature field is compulsory required in order to easily predict the material behavior during the welding process.

Longitudinal weld specifically in thick-walled structures is a common joint type in the fabrication of structural members in the interstate pipeline system. This type of weld joint suffers various types of residual stress fields and deformation patterns, axial and radial shrinkage. These imperfections can have a negative effect on welded structures, which can lead to premature failure. To capture the exact distortion and residual stresses, the calculation methodology based on three-dimensional finite element model for simulating submerged arc welding thick-walled pipes is presented.

The quality of the welding joints and productivity processes used are directly influenced by thermal processes that occur during welding operations accordingly.

Temperature distribution in welded joints is influenced by the linear energy of the heat source, the thermophysical properties of the base material (specific heat, thermal conductibility, material density, thermal diffusivity) and heat loss to the environment.

Based on the analytical solution for the transient temperature field of the semi-infinite body subjected to double-ellipsoidal power density moving heat sources and finite element analysis (FEA), the temperature in the welded steel plates was investigated in the present research.

To model the physics behind the submerged arc welding (SAW) process, a sequentially coupled, full 3D model is employed. Transient, non-linear thermal solution based on heat conduction, convective and radiative boundary conditions is solved in the first part to obtain the nodal temperature history. The temperature fields are further utilized as thermal loads in subsequent elastoplastic structural analysis to obtain the transient and residual stress fields and distortions. The temperature dependent thermo-physical properties such as conductivity, specific heat and density, and temperature dependent thermal–structural properties including Young's modulus, Poisson's ratio, thermal expansion coefficient, yield strength and strain-hardening rate are used for thermal analysis and mechanical analysis, respectively. The metallurgical and mechanical consequences of phase transformation have been

considered in the numerical modeling of the welding process. The analysis is performed by using MSC Marc Mentat, a commercial finite element code enhanced with author written subroutines.

2. FE analysis

For the longitudinal welding of a cylinder with "X" groove, a full 3D FE model along with finite element developed in MSC Marc is shown in Fig. 2. The element type in thermal/structural analysis is SOLID7 (eight-nodes, isoparametric, three-dimensional brick elements with trilinear interpolation. Further details about the selected elements may be found in [17]. High temperature and flux gradients are anticipated in and around the fusion zone (FZ) and heat affected zone (HAZ); therefore, a relatively fine mesh groove, tack weld and root opening in FE model.

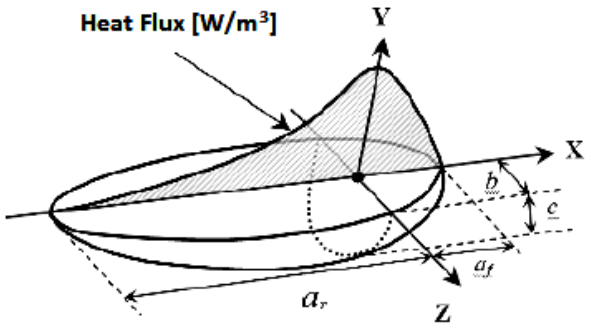

Figure 1: *Double ellipsoidal power density heat source*

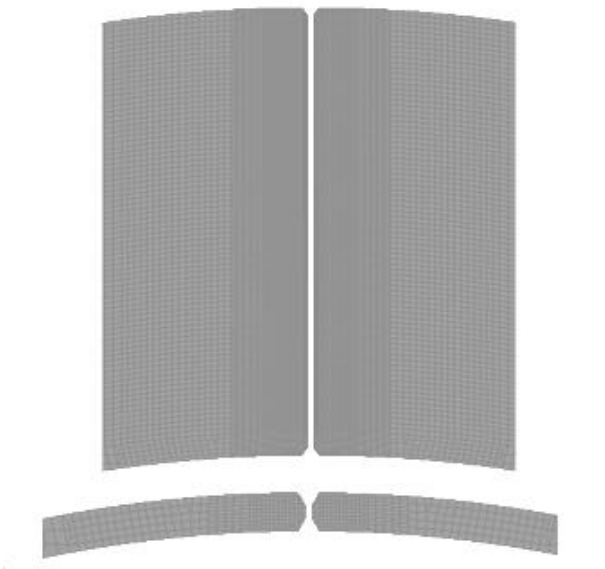

Figure 2: *3D FE mesh based on sensitivity analysis.*

2.1 Thermal analysis technique

A high non-uniform temperature field is generated during the welding process resulting in residual stresses in the welds. The transient temperature distribution is a function of total heat applied and heat distribution patterns within the domain and is highly sensitive to weld-induced residual stresses. A detailed and accurate thermal analysis with appropriate boundary conditions such as heat transfer by conduction, heat losses due to convection and radiation and heat input from the welding torch along with the effects of filler metal deposition, is of paramount importance for the determination of realistic temperature profiles. The governing equation for transient heat transfer analysis during welding process is given by Eq. (1).

$$q_f(x,y,z) = \frac{6\sqrt{3}r_i Q_f}{a_f bc\pi\sqrt{\pi}} exp\left(-\frac{3x^2}{a_f^2} - \frac{3y^2}{b^2} - \frac{3z^2}{c^2}\right) \qquad (1)$$

$$q_r(x,y,z) = \frac{6\sqrt{3}r_i Q_r}{a_f bc\pi\sqrt{\pi}} exp\left(-\frac{3x^2}{a_r^2} - \frac{3y^2}{b^2} - \frac{3z^2}{c^2}\right)$$

The numerical values for heat source parameters used in this paper are: a_f = 10mm, a_r = 25mm, b = 20mm, c = 10mm, in conjunction with the welding process parameters that resulted from experiments.

Flux parameters include the weld power, weld efficiency, an optional scale factor and the dimensions of the flux. The volume weld flux with a double ellipsoidal shape is assumed with the weld width taken as 20mm, the depth of penetration as 10mm, the forward weld length as 10mm and the rear weld length as 25mm. The heat input going into the base metal is taken as 25000W and efficiency is 0.95. Initial position of the heat source is automatically taken as the first point on the associated weld path. The velocity of the weld is taken as 0.0125m/s

The weld path is the path taken by the weld torch as well as the orientation of the torch as it moves along this and a line segment that is parallel to the -Z axis is used to indicate the path.

The deactivated filler element technique in model uses initially deactivated elements that are activated upon physical creation. A thermal activation time of 1e-3 sec is used for ramping up the filler metal temperature.

T_{amb} is taken as 20°C equal to the room temperature.

2.2 Structural analysis technique

The temperature history of each node from the preceding thermal analysis is input as nodal body load in conjunction with temperature-dependent mechanical properties.

Thermo-elastic–plastic material formulation as shown by Eq. (2) [21] with von Mises yield criteria is employed with σ_1, σ_2, and σ_3 being the three principal stresses, coupled to a kinematic hardening rule.

$$\sigma_v = \sqrt{\frac{1}{2}[(\sigma_1 - \sigma_2)^2 + (\sigma_2 - \sigma_3)^2 + (\sigma_3 - \sigma_1)^2]}. \quad (2)$$

4. Results and discussion

4.1 Thermal analysis

The temperature at different time steps (t=30 and 70s) - when two thermal sources are applied on the top surface of the joint, obtained using the deactivated element techniques is shown in Figs. 3 and 4.

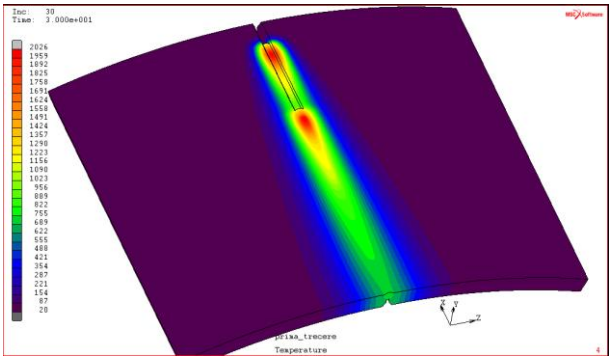

Figure 3: Temperature field at t=30s (Top Surface)

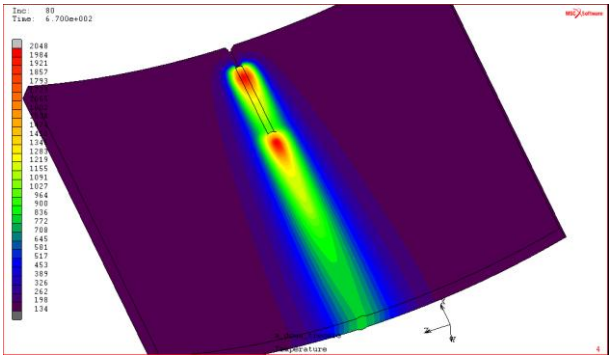

Figure 4: *Temperature field at t=70s (Bottom Surface)*

More relevant are the temperature charts plotted both on top and bottom of joint for each case simulated, illustrated in Fig. 5. Peak temperature decreases with distance increasing. On the other side (bottom) of joint, the temperatures are slightly higher and decrease from 2041°C. This slight increase is the effect of welding performed on top surface and seems to be similar to a preheating leading to a decrease of cooling speed. Preheating is a common practice in welding high-strength steels, because it reduces the risk of heat-affected zone cracking. Higher welding speeds lead to higher cooling rate and, further to the finer cells, while at lower welding speeds the cooling rate is lower and the cells are coarser.

The temperature variation with time at different points of the structure is shown in Fig. 6. The results are obtained for four nodes: node 80278 is a filler element node; node 25094 is a base metal node at the junction of the weld filler and base; node 25115 is a base metal node in the heat affected zone; and base metal node 24114 is far away from the weld.

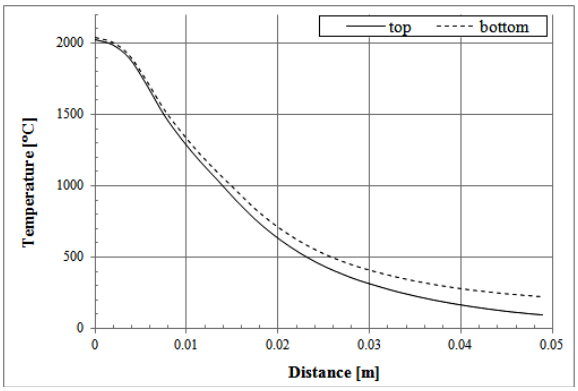

Figure 5: *Temperature profile in cross section vs. distance between welding sources*

The node corresponding to the filler element (node 80278) is at 20°C during the deactivated stage and it rises over to melting point over the ramp time of 1e-3 sec and remains at this temperature during the time it remains in the weld pool. The approximate time period for the time it remains in the weld pool can be estimated as = (weld pool length)/(weld velocity) = (.025 + .01)/.0125 = 2.8 seconds.

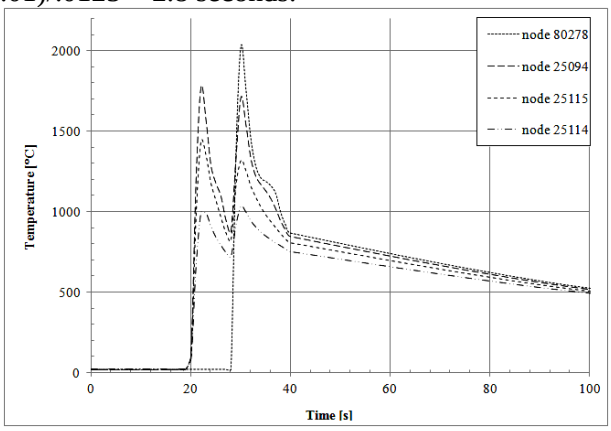

Figure 6: *Temperature variation with time at different filler and base metal locations*

4.2 Stress analysis

The residual Von Mises stresses obtained using the deactivated filler element techniques are shown in Figs. 7 and 8 respectively.

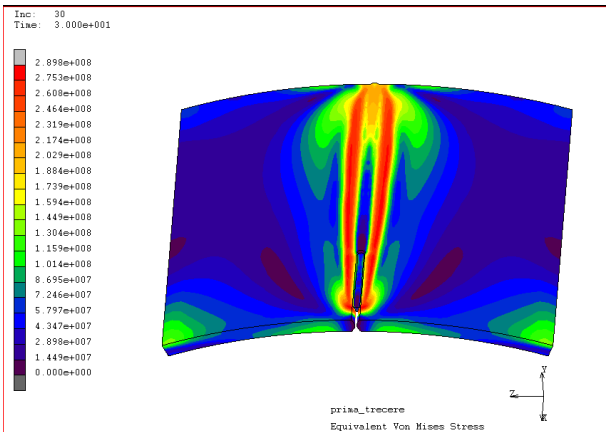

Figure 7: *Von Mises stress at t=30s (Top Surface)*

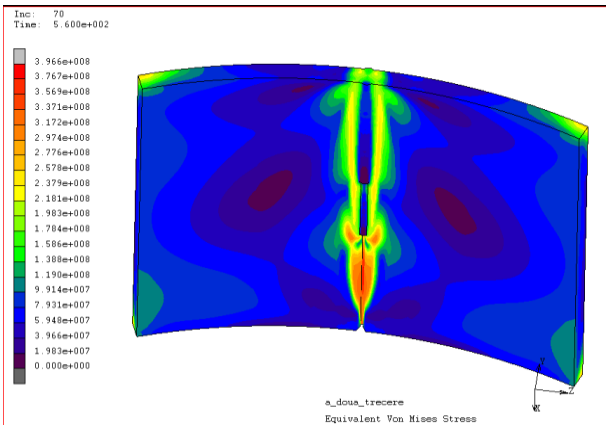

Figure 8: *Von Mises stress at t=70s (Bottom Surface)*

The Von Mises stress is attributed to different temperature profiles on the inner and outer surfaces of the cylinders. The shrinkage patterns due to different temperature gradients, near the weld line (WL), make to appear the tensile and compressive residual stress fields on inner and outer surfaces, respectively.

Fig. 9 show the Von Mises stress distribution for five different times during the welding process. Von Mises residual stresses are symmetric due to symmetry across the WL.

The low Von Mises stress approach a zero value in weld pool and near the fusion zone (FZ) high stresses are predicted.

As observed, HAZ zone begins at 20mm from WL and the width is approximately 30mm. The peak residual Von Mises stress is 282MPa.

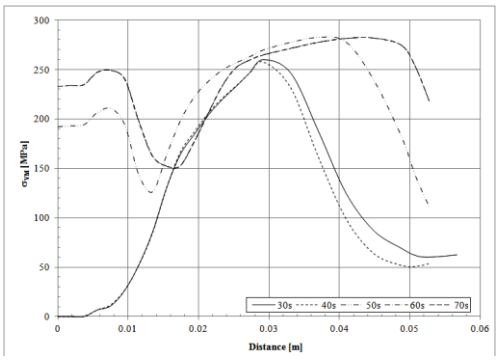

Figure 9: *Von Mises stress profile in cross section vs. distance between welding sources at different moment of time*

5 Acknowledgement

This work was supported by a grant of the Romanian National Authority for Scientific Research, CNDI– UEFISCDI, project number PN-II-PT-PCCA-2011-3.1-1057.

6 References

[1] Birsan D., Rusu C., Scutelnicu E., Mistodie L., *Heat Transfer Analysis in API X70 Steel Joints Performed by Double Submerged Arc Welding*, Conferinta ROMAT 2012.

[2] Birsan D., Scutelnicu E., *Stress and temperature field modelling at web stiffeners welding*, The Annals of Dunarea de Jos University of Galati, Fascicle XII, Welding Equipment and Technology, Year XXI, 2011, ISSN 1221 4639, pag.15-19.

[3] Goldak, J., Chakravarti A. and Bibby M., *A new finite element model for heat sources*, Metallurgical Transactions B, vol. 15 B, pp. 299-305, 1984.

[4] Goldak J., Bibby M., Moore J., House R., Patel B., *Computer modelling of heat flow in welds*, Metallurgical Transactions B, vol. 17 B, 1986, pp. 587-600.

[5] Goldak J., Zhou J., Breiguine V., Montoya F., *Thermal stress analysis of welds: from melting point to room temperature*, JWRI, vol. 25, No. 2, pp. 1851-89, 1996.

[6] Sabapathy P. N., Wahab M. A., Painter M. J., *Numerical models of in service welding of gas pipeline*, Journal of Materials Processing Technology, vol. 118, 2001, pp. 14-21.

[7] Ravichandran G., Raghupathy V. P., Ganesan N., *Analysis of temperature distribution during circumferential welding of cylindrical and spherical components using the finite element method*, Journal of Computer and Structures, vol. 59, No. 2, 1996, pp. 225-255.

[8] Ueda Y., Yamakawa T., *Analysis of thermal-elastic stress and strain during welding by finite element method*, JWRI, vol. 2, No. 2, 1971.